Analysis of electric signals of rock beams subjected to bending

P. Kyriazis[1, 2] C. Anastasiadis[1], I. Stavrakas[1], D. Triantis[1], J. Stonham[2]

1. Technological Educational Institution of Athens, Department of Electronics, Athens, Greece
2. Brunel University, School of Engineering and Design, Uxbridge, United Kingdom

ABSTRACT

Experimental laboratory work has been conducted to study electric signals of marble beams that have been subjected to three point bend tests. The specimens have suffered 12 abrupt loading steps up to failure and the corresponding BSC were recorded by means of copper electrodes placed in the lower surface of the sample. Alongside with the application of abrupt loading to the samples, BSC peaks were observed and then the current followed an exponentially decreasing relaxation process. In this paper the BSC peaks, the total charge, as well as the characteristic relaxation time variables are correlated with each other and also with the applied loading. The ultimate purpose is the evaluation of the fatigue of the sample using simple criteria.

1. INTRODUCTION

Rocks and especially marble was broadly used in the past as a construction material in monuments and buildings. A typical example of such a monument is the Parthenon temple of Acropolis of Athens. Acropolis monuments have suffered botched earlier restorations as well as corrosion and fatigue as they stand there for centuries. Today restoration works are in progress aiming to save Acropolis basically from present day environmental hazards. Therefore it is important to evaluate Non-Destructive Testing techniques that will allow the continuation of the restoration works and the evaluation of the fatigue of the marbles so as to avoid all possible hazards.

The proposed method is based on electric phenomena that accompany mechanical stress of rocks. It has been observed that when deformation of a rock sample occurs, the sample reacts by emitting electric current (Brady and Rowell, 1986; Enomoto and Hashimoto, 1990; Hadjicontis and Mavromatou, 1994; Takeuchi and Nagahama, 2001; Freund, 2002). Laboratory experiments including many fracture tests have been conducted on various minerals and rocks both dry and saturated in order to understand and interpret the nature of the mechanisms responsible for the production of such electrical signals (Yoshida et al., 1998; Vallianatos et al., 2004; St-Laurent et al., 2006).

In our previous work construction materials were tested against loading of bending type up to fracture and failure (Triantis et al., 2006). The emitted electric signals were given the name "Bending Stimulated Currents" and were partially attributed to mechanisms consistent with the MCD model (Vallianatos et al., 2004). In this paper a further attempt to understand and analyse the recorded electric signals is presented, having as reference for the explanation of phenomena the work by Anastasiadis et al. 2007.

2. EXPERIMENTAL PROCEDURE

2.1 Material under examination

In this section marble, which is the material under examination, is described. Rock materials and especially marble have been used in the past in constructions and therefore results concerning their strength may serve in many restoration works that are in progress as for example on the Parthenon temple of Acropolis of Athens as well as on other civil engineering applications.

Marble is a geomaterial of known physical and chemical properties, which have been thoroughly presented in the previous works. The marble samples under examination were collected from Mt. Penteli (Dionysos) and are mainly composed of calcite (98%) and other minerals i.e. 0.5% of muscovite, 0.3% of sericite, 0.1% of chlorite, it also contains 0.2% of quartz (Kourkoulis et al. 1999). Its specific density is 2730 kg/m^3, its apparent density is 2717 kg/m^3 and its porosity is very low, varying from 0.3% for pristine marble to 0.7% for marble that has suffered natural weathering and has been exposed to corrosive agents (Kleftakis et al. 2000). The dimensions of the beam specimens were 40mm x 40mm x 150mm and their fracture limit was 30kN.

2.2 Experimental setup

In this section the experimental setup used for the characterization of the material is described. In Figure 1 the testing arrangement and the geometry of the tested marble is presented. The beam of marble is supported by two prism-like wedges in two points and stressing forces are applied in the middle of the sample so as to emulate typical bending conditions. Special attention was paid to get proper and symmetric geometry, as it is a key point in a three point bending experiment as far as the failure plane is concerned.

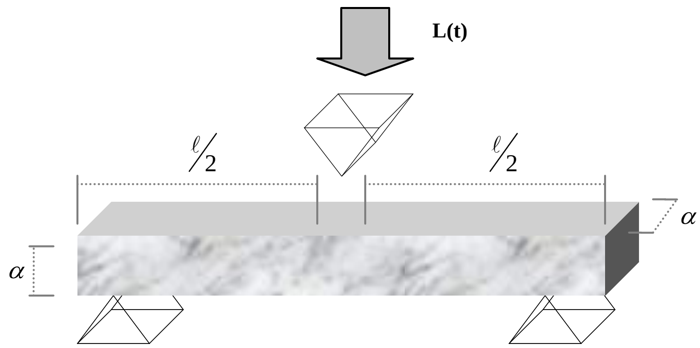

Figure 1. Marble beam geometry and loading

Experimental setup is precisely presented in Figure 2, which includes both the mechanical parts that perform application of the load as well as the electronic setup that is used for the recording of the BSC measurements. The system comprised a uniaxial

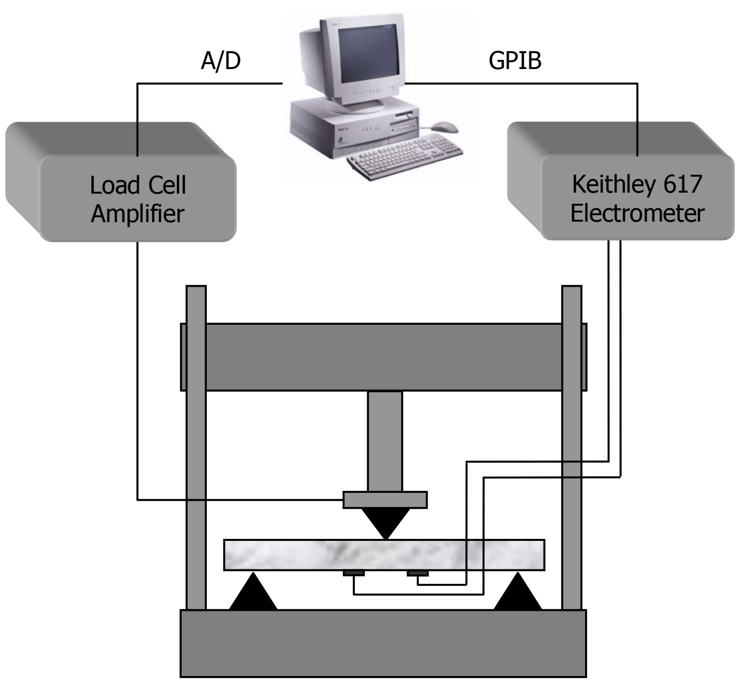

Figure 2. Mechanical and electronic setup for conducting BSC experiments

hydraulic load machine (Enerpac-RC106) that was used to apply loading, while the whole setup was placed on a stainless steel base. The values of the externally applied stress were recorded using a manometer.

A pair of electrodes is positioned on the lower surface of the beam (see Fig.2) and the BSC measurements are achieved using a sensitive programmable electrometer (Keithley 617) with current range from 0.1fA to 20 mA. Each set of measurements is transferred to a PC through GPIB interface and is stored in the hard disk. The experiments are conducted in a Faraday shield to prevent measurements from being affected by ambient electric noise.

The adopted technique for the loading of the samples in the experiments is based on the increase of the load with abrupt steps and it is implemented as follows. The beam which is under testing is initially subjected to loading of a constant value L_k. An abrupt stepwise load increase of short duration Δt is applied so that the load increases by $\Delta_L = L_{k+1} - L_k$, where L_{k+1} is the new state, after the application of the load increment. It must be noted that the new stress level L_{k+1} remains constant until the application of a further load increment. The aforementioned temporal variation of load L, as recorded during this experimental procedure can be described in a good approximation by the following equation (1).

$$L(t) = \begin{cases} L_k = \text{constant} & \text{for } t<t_k \\ L_k + b(t-t_k) & \text{for } t_k<t<t_{k+1} \\ L_{k+1} = \text{constant} & \text{for } t>t_{k+1} \end{cases} \quad (1)$$

Typical value of the loading rate b in the moments of the increase of the applied loading is about 0.2kN/s.

3. EXPERIMENTAL RESULTS

3.1 Signal recordings

The conducted experiments are three point bending tests of marble beams, which mechanical and physical properties were described in previous section. In Figure 3 the evolution of the experiment is depicted. The applied loading L with respect to time and the corresponding recorded current are presented. The current is referred as Bending Stimulated Current (BSC) for compliance with the term Pressure Stimulated Current

(PSC), which is used for the current yielding from stressed samples. In Figure 3 can be seen that the loading remained constant after each loading step in order to allow for the current to relax to the initial background values. The recorded BSC is presented in a semi-log graph for better visualization of both high and lower current peaks as well as of the micro fluctuations in the relaxation process of the final steps. The selection of the time interval of each loading step is based on the relaxation time of the relaxation process of the BSC (i.e. the time that is needed for the BSC to relax to background level) and therefore time interval between successive steps is not constant as shown in Figure 3.

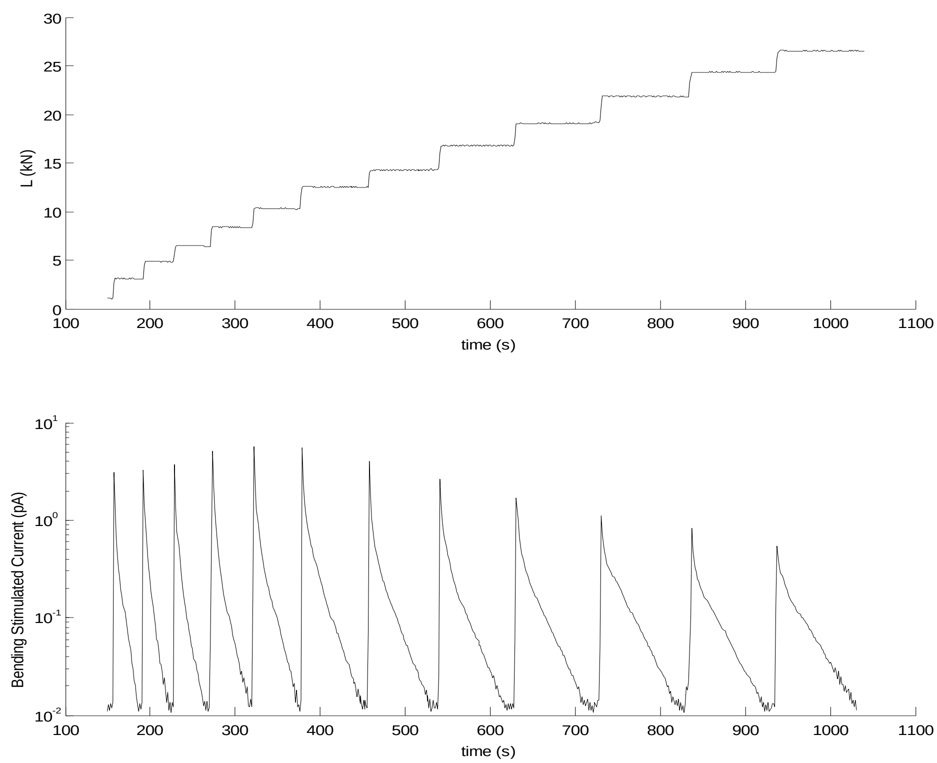

Figure 3. (a) Loading steps (b) Weak electric current (BSC) recordings

The occurrence of electric current can be correlated with the loading rate (dL/dt) which is depicted in Figure 4, as the deviation in the loading rate coincides temporally with the occurrence of a BSC peak. However, the actual value of the BSC peak varies from one loading step to the other, although the value of peak loading rate is the same for every step i.e. 1kN/s. Note that in Figure 4 the recorded BSC is the same as in Figure 3, but its scale is linear instead of logarithmic.

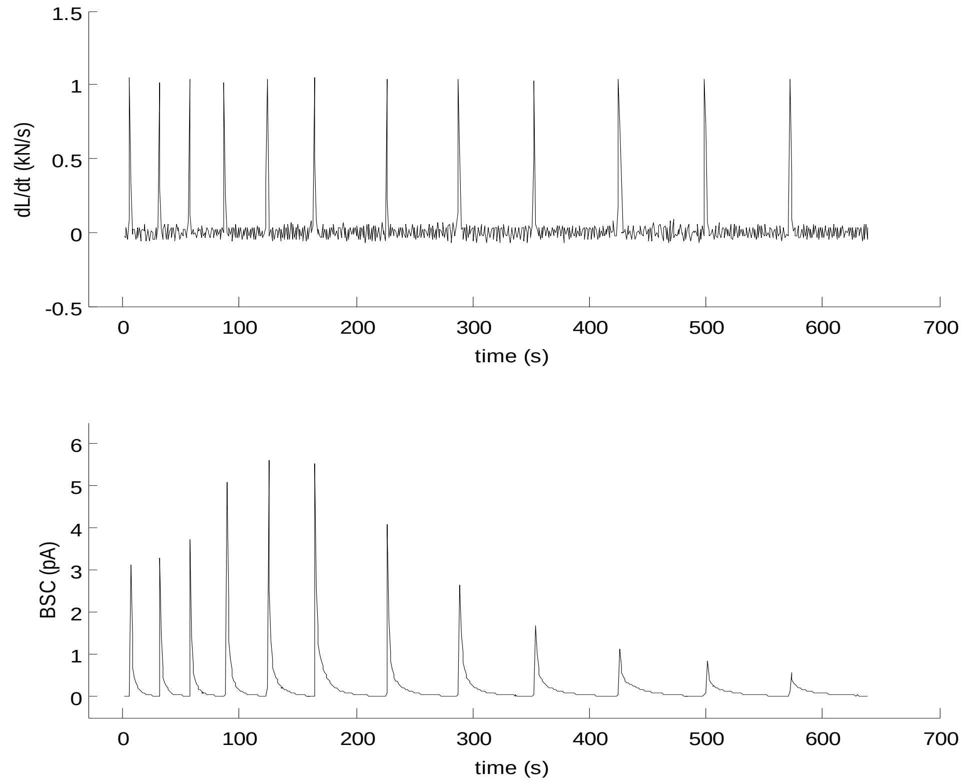

Figure 4. (a) Stress rate variation in the experiment (b) Weak electric current (BSC) recordings

3.2 Signal analysis

In this section an attempt to further analyze the signal and extract useful information that will serve for the interpretation of phenomena following fracturing of the marble is presented. The 3 point bend tests lead the marble beams to fail at a certain plane parallel to the loading direction. In case of U or V notched beams the crack position and direction can be predicted in a more robust way, however in these experiments the beams were selected to be pristine, so as to emulate typical conditions of construction applications. All samples failed in the middle, towards a plane initiating at the point where the upper wedge is positioned.

The current peak corresponding to each loading level and therefore to each loading step is a parameter that can be correlated with the fatigue of the sample and the severity of damage at each loading level. In Figure 5 two parameters are presented in a unified plot. The x-axis represents the normalized loading level loading step and the y-axis the normalized values of the BSC peaks and the value of the total recorded charge that corresponds to each loading level and thus to each loading step process.

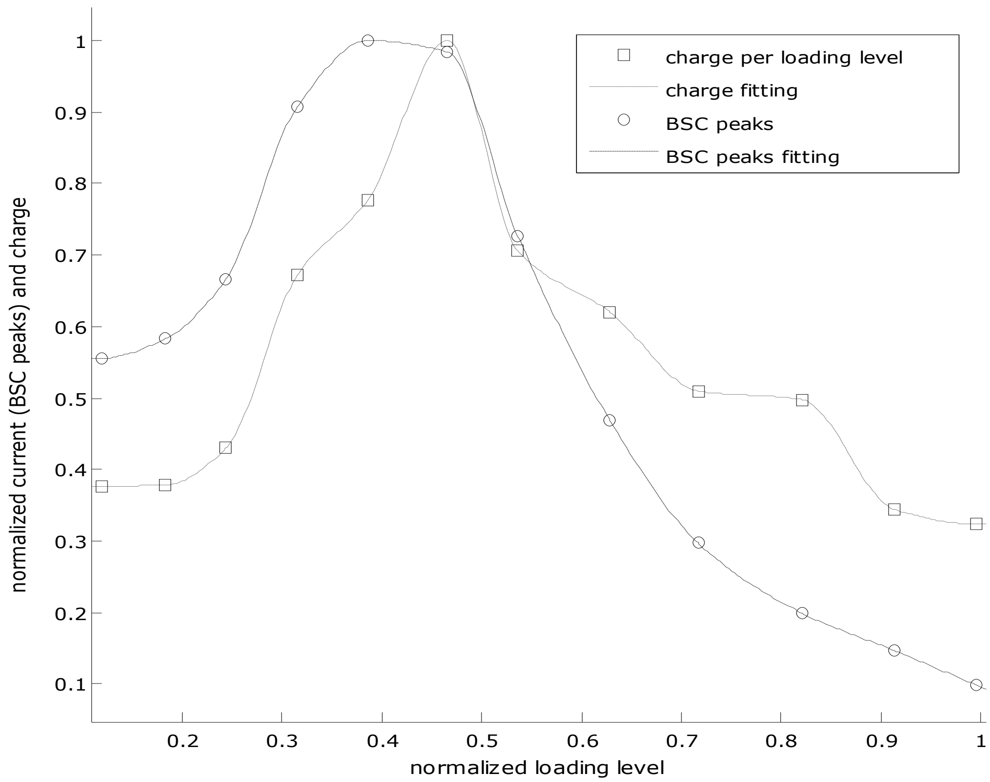

Figure 5. Normalized BSC peaks and normalized total charge flow past the electrodes at each loading level that corresponds to each loading step

The BSC peaks have been fitted using shape-preserving spline fit. More specifically the Piecewise Cubic Hermite Interpolation Polynomial (PCHIP) has been selected instead of typical spline fitting, as it preserves the shape of data and it respects monotonicity.

Subsequently the complete BSC recording was fitted using PCHIP, because of a key property of this fitting type, which is that it has no overshoots and exhibits less oscillation, when applied to non-smooth data such as the BSC recordings. The total charge that flows past the electrodes that are placed on the beam, during each loading step can be calculated. The finite integral of the fitted BSC recordings, having as lower limit the time of the application of the stress step and as upper limit the moment of the application of the next stress step, corresponds to the total charge of each step, as the rate of the charge flowing past a certain plane is the recorded electric current. Equation 2 has been used to calculate the charge.

$$Q_{n\_step} = \int_{t_n}^{t_{n+1}} BSC(t)dt \qquad (2)$$

The normalized flowing charge is an important parameter to evaluate, as it can serve as a metric of the amount energy that corresponds to each fracture stage, mainly because it combines both current and time interval of the relaxation process. In other words the current peak and the duration of the current relaxation process that follows are combined and expressed through the charge. A typical example showing the aforementioned facts is that the BSC peak graph exhibits maximum earlier compared to charge maximum. Furthermore it is observed that in the last loading steps where the current peaks are significantly lower the total charge remains relatively high because the relaxation processes are slower.

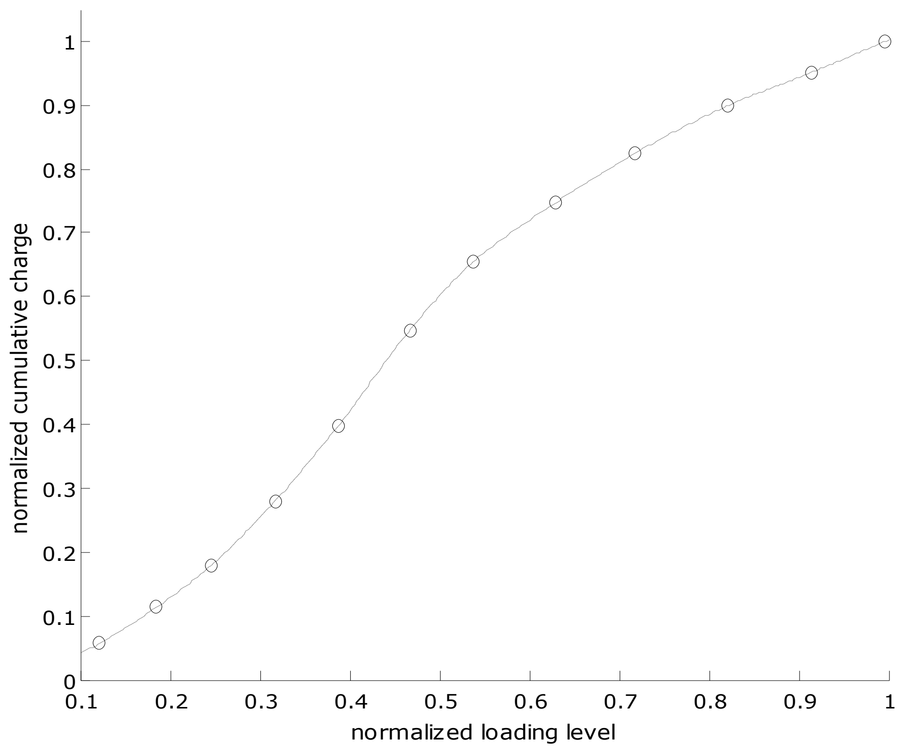

Figure 6. Normalized cumulative charge with respect to loading levels at each loading step.

In Figure 6 we present the cumulative distribution of the charge with respect to the normalized loading levels. The loading increases following an almost linear law while the charge does not increase linearly. It increases quickly up to loading level 0.5 and then the increasing rate drops, thus a saddle point for the charge graph appears which may serve as criterion of the fatigue of the sample. The saddle point of the charge graph is a precursory of the fracture of the sample which appears early enough (at half the strength of the sample) and may help to predict ahead of time the failure of a bended beam. Talking in terms of system analysis, we may consider the loading as the input of a system and the total charge as its output. The two parameters cannot be correlated linearly which is an indication of a non-linear and dynamic system.

In previous work the relaxation process has been separated into two parts, since after the appearance of PSC_{max} the current starts relaxing down to background level, at an initially fast rate and a slower one after a certain point that the slow relaxation mechanism becomes dominant. The relaxation processes that follow a fairly slow rate were examined and have been modeled with Equation 3.

$$PSC(t) = A \cdot \exp\left(-\frac{t}{\tau}\right) \tag{3}$$

where A is a factor and τ a time parameter which is characteristic for each relaxation process. The slow relaxation processes have been fitted using the exponential law presented in Equation 3 and the results of the calculated parameter τ are shown in Figure 7 for normalized loading levels.

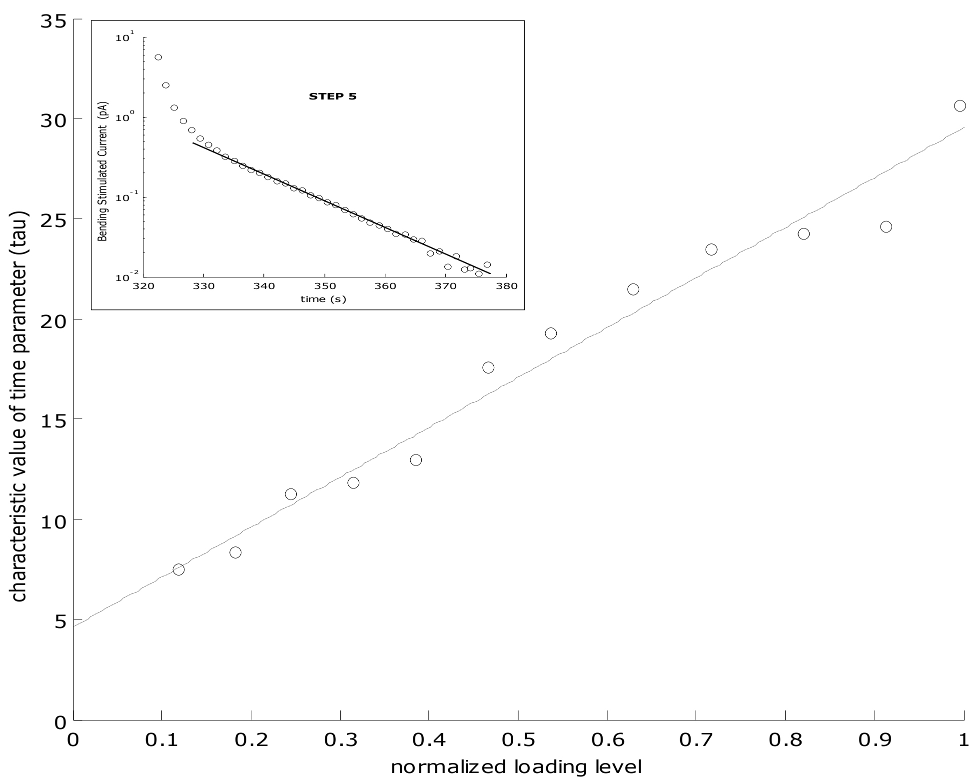

Figure 7. Linearly fitted characteristic time parameter τ of slow relaxation processes of the BSC corresponding to each loading level

A probable cause of the appearance of the second (slow) relaxation mechanism process is the continuing material strain, even at a very low rate, although stress is unchanged. The new microcracks that go on appearing produce new microcurrents and result in conserving PSC at relatively high values that do not permit a direct relaxation to noise level. Therefore the increase of relaxation time is a parameter depicting the ageing of the sample beams and the damage they have suffered.

4. DISCUSSION

In this section we discuss about the modelling of current peaks with respect to the cracking mechanisms that are involved in our experiments. The bending of the beam has been implemented experimentally as presented in previous section by a 3-point test. The beams were led to fracture and failure which has been observed towards a certain plane parallel to the direction of the applied force to the upper wedge of the 3point bend setup. However, the failure plane observed here has not been created by one main crack as happens in the case of compressional stress tests where one main crack propagates creating a shearing plane (R.J. Sanford, 2003). In the bending tests there are two regions of the beam that behave in a different way. The upper part of the beam is mainly subjected to compression, while the lower part of the beam to tension. Therefore, two distinct cracks one from the top and one from the bottom propagate and both tips of the cracks move towards the centre of the beam.

The recorded current is a transient one and its nature and properties has been explained and examined in previous work in the frame of MCD model (Vallianatos et al., 2004). In compressional tests the electrodes were perpendicular to the axis of the loading and therefore the component of the current that flowed through electrodes surface was recorded. In the case of bend, because of the existence of two fracturing mechanisms and thus of two cracks propagating in opposite directions the measured current is the superposition of the currents that are created in the tip of each crack because of the bonds' breaking.

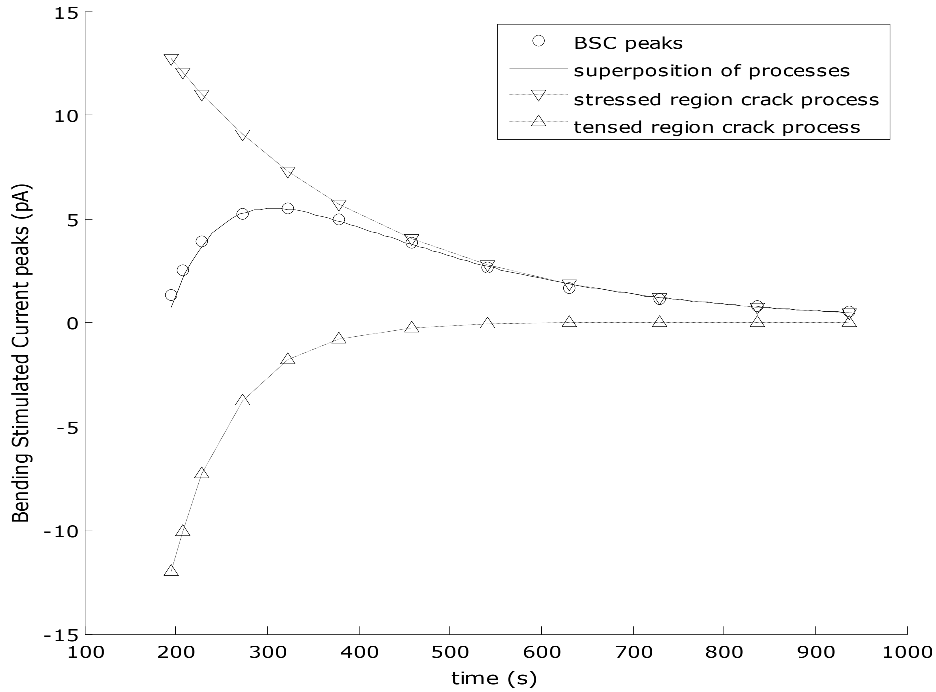

Figure 8. BSC peaks interpretation as a superposition of distinct processes i.e. the tension process and the compression process

In this way it can be explained why in bend test the current peaks do not follow an exponential decrease, but two different exponential processes expressed with Equation 4.

$$\mathrm{BSC}_{peak}(t) = A_{comp} e^{-\frac{t}{\tau_{comp}}} - A_{tens} e^{-\frac{t}{\tau_{tens}}} \tag{4}$$

Bearing in mind that in the compressed region of the beam suffers less damage compared to the tensed region of the beam it the relation between the two characteristic parameters of the exponential processes (i.e. $\tau_{\mathrm{comp}} > \tau_{\mathrm{tens}}$) is a presumed result.

In Figure 8 the two mechanisms compression for the upper part of the beam and tension for the lower part obviously follow the exponential decrease known from earlier work (Kyriazis et al., 2006). However their superposition yields the BSC peaks graph shown also in Figure 8. The two processes exhibit different characteristics as far as the rate of decrease of the BSC peaks is concerned owing to the different rates of damage of the two regions (i.e. tended region crack propagates more quickly compared to the compressed region crack) and that is why the superposition of the current peaks is not constant during the whole experiment. Finally we should note that the two processes graphs yield as the best fits of the recorded BSC peaks data and are not actually measured parameters as in our method the source of the measured current is not specified. In the future acoustic emission measurements would be useful to verify our model for bending.

5. CONCLUSIONS

In this work 3-point bend tests on marble beams, that aim to investigate a weak electric current emission based non-destructive technique, are presented. were presented and explained. The total charge flowing from electrodes was selected to create a criterion of fatigue. The saddle point of the curve of the cumulative recorded charge appears almost at half strength of the beams and may serve as a criterion for a non-destructive method. The relaxation process of the current for each loading step was separately analysed and the characteristic relaxation times increase linearly. Thus relaxation time is another parameter that shows the fatigue of the material that is subjected to bending. Finally the recorded BSC peaks were modelled as a superposition of two distinct mechanisms, the first corresponding to the tensed region of the beam and the second to the compressed region accordingly.

REFERENCES

Anastasiadis, C., Triantis & Hogarth C. A. (2007), Comments on the phenomena underlying pressure stimulated currents in dielectric rock materials, Journal of Materials Science, vol.42, 8, pp 2538-2542

Brady, B. T. and Rowell G. A. (1986), Laboratory investigation of the electrodynamics of rock fracture, Nature, 321, pp. 488–492.

Enomoto, J. and Hashimoto H. (1990) Emission of charged particles from indentation fracture of rocks, Nature, 346, pp. 641–643.

Freund, F. (2002), Charge generation and propagation in rocks, J. Geodyn, vol. 33, pp. 545–572.

Hadjicontis, V. and Mavromatou, C. (1994) Transient electric signals prior to rock failure under uniaxial compression, Geophys. Res. Lett., 21, pp.1687–1690.

Kourkoulis, S.K., Exadaktylos, G.E., and Vardoulakis I.(1999). U-notched Dionysos-Pentelicon marble beams in three point bending: The effect of nonlinearity, anisotropy and microstructure. International Journal of Fracture, 98, pp. 369-392.

Kyriazis, P., Anastasiadis, C., Triantis, D. and Vallianatos, F (2006) Wavelet analysis on pressure stimulated currents emitted by marble samples. Natural Hazards and Earth System Sciences, vol.6, pp. 889-894.

Sanford R.J. (2003) Principles of Fracture Mechanics, Prentice Hall

Takeuchi, A. and Nagahama, H. (2001), Voltage changes induced by stickslip of granites, Geophys. Res. Lett., 28, 3365–3368.

Triantis, D., Anastasiadis, C., Kyriazopoulos, A., Kyriazis, P., & Alexis N. (2006), Electric current emissions during bending of FRP samples up to fracture, Proc. 2nd Intern. conf. Advances in Mineral Resources Management and Environmental Geotechnology pp. 425-430.

Vallianatos, F., Triantis, D., Tzanis, A., Anastasiadis, C., and Stavrakas, I. (2004), Electric Earthquake Precursors: From Laboratory Results to Field Observations, Phys. Chem. Earth, 29, pp. 339–351.

Yoshida, S., Clint, O. C., and Sammonds, P. R. (1998), Electric potential changes prior to shear fracture in dry and saturated rocks, Geophys.Res. Lett., 25, pp. 1577–1580.